Brain Receptor Imaging*

Wolf-Dieter Heiss, MD[1]; and Karl Herholz, MD[2]

[1]*Max-Planck Institute for Neurological Research and Department of Neurology, University of Cologne, Cologne, Germany; and*
[2]*Wolfson Molecular Imaging Centre, University of Manchester, Manchester, United Kingdom*

Receptors have a prominent role in brain function, as they are the effector sites of neurotransmission at the postsynaptic membrane, have a regulatory role on presynaptic sites for transmitter reuptake and feedback, and are modulating various functions on the cell membrane. Distribution, density, and activity of receptors in the brain can be visualized by radioligands labeled for SPECT and PET, and the receptor binding can be quantified by appropriate tracer kinetic models, which can be modified and simplified for particular application. Selective radioligands are available for the various transmitter systems, by which the distribution of these receptors in the normal brain and changes in receptor binding during various physiologic activities or resulting from pathologic conditions can be visualized. The quantitative imaging for several receptors has gained clinical importance—for example, dopamine (D_2) receptors for differential diagnosis of movement disorders and for assessment of receptor occupancy by neuroleptics drugs; serotonin (5-hydroxytryptamine, 5-HT) receptors and the 5-HT transporter in affective disorders and for assessment of activity of antidepressants; nicotinic receptors and acetylcholinesterase as markers of cognitive and memory impairment; central benzodiazepine-binding sites at the γ-aminobutyric acid A ($GABA_A$) receptor complex as markers of neuronal integrity in neurodegenerative disorders, epilepsy, and stroke and as the site of action of benzodiazepines; peripheral benzodiazepine receptors as indicators of inflammatory changes; opioid receptors detecting increased cortical excitability in focal epilepsy but also affected in perception of and emotional response to pain; and several receptor systems affected in drug abuse and craving. Further studies of the various transmitter/receptor systems and their balance and infraction will improve our understanding of complex brain functions and will provide more insight into the pathophysiology of neurologic and psychiatric disease interaction.

Key Words: receptor binding; radioligands; PET; SPECT; dopamine; serotonin; cholinergic receptors; benzodiazepine-binding sites; opioid receptors; adenosine receptors

J Nucl Med 2006; 47:302–312

Receptors are structures, usually proteins, on cellular membranes that, after interaction with specific ligands (first messenger transmitters), trigger a signal causing defined responses mediated by secondary messengers (G-protein–coupled receptors) or ion channels (ligand-gated ion channels) (*1*). Receptors can be characterized by their affinity and density; as proteins, they are degraded after a functional period by specific proteases. The function of receptors is obvious in direct neurotransmission, where the interaction of a presynaptically released transmitter with the postsynaptic receptor causes depolarization or hyperpolarization of the postsynaptic membrane. Receptors can also be located on the presynaptic membrane—important for negative feedback and for reuptake of transmitters—and on cell bodies. Receptors involved in direct neurotransmitter function are found in high density in specific brain areas and are affected by many pathologic conditions; therefore, they form a primary target for imaging studies. Other receptors have a modulating effect on signal transduction. They can affect cell membrane enzymes and transcription factors of protein-coding genes. These receptors are distributed in lower density and their in vivo detection is still limited but might gain importance in the future. Imaging of the regional distribution of receptors provides a relevant insight into the organization of functional networks in the brain, which cannot be achieved by morphologic investigations or imaging of blood flow and metabolism. It must be kept in mind that histochemical receptor studies have demonstrated a complex laminar distribution of several receptor types in individual cortical areas, which contribute to the neurochemical organization of intracortical and cortical–subcortical networks (*2*). This multireceptor organization of functional networks can only be visualized by postmortem autoradiography but is not accessible for in vivo imaging studies.

Distribution, density, and activity of receptors in the brain can be visualized and quantified by radioligands (Table 1), which must fulfill several criteria to be successful for PET or SPECT (*3,4*): stability of labeling; sufficient affinity and high selectivity for the specific receptor combined with low nonspecific binding to brain tissue not containing the receptor of interest; rapid permeation through the blood–brain barrier permitting high access of tracers to receptors. Additionally, there should be as few as possible metabolites

Received Jul. 29, 2005; revision accepted Oct. 18, 2005.

For correspondence or reprints contact: Wolf-Dieter Heiss, MD, Max-Planck Institute for Neurological Research, Gleueler Strasse 50, 50931 Köln, Germany.

E-mail: wdh@pet.mpin-koeln.mpg.de

*NOTE; FOR CE CREDIT, YOU CAN ACCESS THIS ACTIVITY THROUGH THE SNM WEB SITE (http://www.snm.org/ce_online) THROUGH FEBRUARY 2007.

TABLE 1
Selected Receptor Tracers

Tracer	Abbreviation	Target
^{11}C-Cocaine, ^{11}C-methylphenidate		DAT
^{11}C-Nomifensine		DAT
^{11}C-WIN-35428, ^{11}C-PE2I		DAT
^{18}F-2β-Carbomethoxy-3β-(4-fluorophenyl)tropane	CFT	DAT
^{11}C-Dihydrotetrabenazine	DTBZ	$VMAT_2$
^{11}C-SCH-23390		D_1
^{11}C-*N*-Methylspiperone	NMSP	D_2, 5-HT_2
^{18}F-*N*-Methylspiperone		
^{18}F-Fluoroethylspiperone	FESP	D_2, 5-HT_2
^{11}C-Raclopride	RAC	D_2
^{18}F-Fallypride		D_2
N-1-^{11}C-Propylnorapomorphine		D_2 (agonist)
^{11}C-L-Deprenyl		MAO-A
^{11}C-*N*-Methyl-4-piperidylbenzilate	NMPB	Muscarinic receptors
N-^{11}C-Methylpiperdin-4-yl-propionate	MP4P, PMP	AChE
N-^{11}C-Methyl-4-piperidyl-acetate	MP4A, AMP	AChE
^{11}C(+)-McN5652		5-HTT
^{11}C-3-Amino-4-(2-dimethylaminomethyl-phenylsulfanyl)benzonitrile	DASB	5-HTT
^{11}C-WAY-100635	WAY	5-HT_{1A} receptor
^{18}F-Altanserin		5-HT_{2A} receptor
^{11}C-Flumazenil	FMZ	$GABA_A$/benzodiazepine receptors
^{11}C-PK-11195	PK	Peripheral benzodiazepine receptors
^{11}C-Carfentanyl		Opioid μ receptor
^{11}C-Diprenorphine	DPN	Opioid receptors
^{18}F-Cyclofoxy		Opioid receptors
^{18}F-CPFPX, ^{11}C-MPDX		Adenosine A_1 receptor

DAT = dopamine transporter; VMAT2 = vesicular monoamine transporter type 2; D1 = dopamine 1 receptor; D2 = dopamine 2 receptor; 5-HT = 5-hydroxytryptamine (serotonin) receptor; 5-HTT = 5-hydroxytryptamine (serotonin) transporter; MAO-A = monoamino-oxidase A; AChE = acetylcholinesterase; GABA = γ-aminobutyric acid receptor.

of labeled ligand. If metabolites are generated in brain tissue, concentrations should be low with rapid clearance, whereas systemic metabolites present in plasma should be polar so that they cannot cross the blood–brain barrier and enter the brain.

IMAGING AND QUANTITATIVE ANALYSIS OF RADIOLIGAND STUDIES

Radioligand studies permit measurement of the time course of uptake and clearance of specific tracers but, for the assessment of pharmacokinetic parameters from these time–activity curves, a tracer kinetic model is needed, which usually requires an input function indicating delivery of tracer to the tissue. In some applications for receptor studies, an arterial input function can be replaced by a reference to tissue devoid of specific binding sites (*5–11*). At present, PET represents the most selective and sensitive (pico- to nanomolar range) method for measuring receptor density and interactions in vivo. For many receptor studies, SPECT can also be applied but detector efficiency is much lower and it provides less quantitative accuracy than PET. SPECT isotopes typically have longer physical half-lives than most PET tracers, which may partially compensate for their disadvantages if measurement times over several hours are required to get rid of nonspecific binding and reach equilibrium.

Imaging of radioligand distribution at some stage after intravenous injection shows the pattern of relative uptake in different regions. In some instances, this pattern represents receptor density but usually the regional signal does not only represent specific receptor binding but also contains contributions from nonspecific binding, free ligand in tissue, and intravascular activity, and all these components vary with time after tracer injection. Therefore, kinetic studies are necessary to differentiate the various components and to extract the compartment of specific binding. This implies acquisition of multiple scans for measuring cerebral uptake, clearance of the tracer, and assessment of the tracer concentration in arterial plasma over a period of 30–120 min. In addition, with some tracers metabolites must be measured for correction of plasma curves.

DETERMINATION OF RECEPTOR BINDING

For the determination of the dynamics of receptor binding, a 3-compartmental model (Fig. 1) can be applied, with the free exchangeable ligand in plasma, the free-to-bind ligand in tissue, and the specifically bound ligand forming the compartments and kinetic constants describing the interaction among

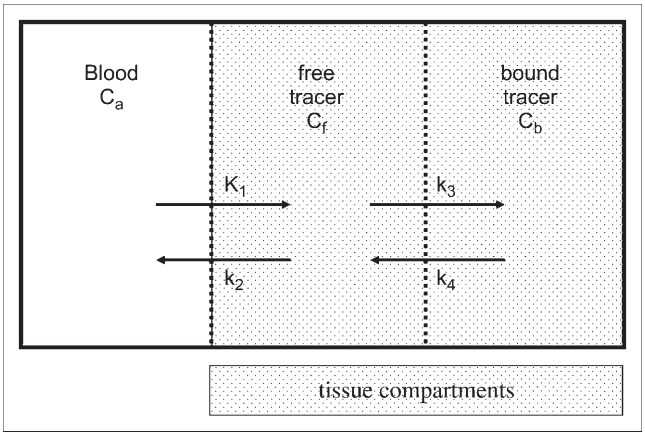

FIGURE 1. Standard compartmental model for receptor-binding ligands. C_a, C_f, and C_b represent time-dependent local activity of tracer in blood and free and bound tracer in tissue, respectively. K_1 to k_4 are the transfer rate constants between compartments.

these compartments. Differential equations describe the change of concentrations in these compartments over time:

$$dC_f/dt = K_1 \cdot C_a - (k_2 + k_3)C_f + k_4 \cdot C_b$$

and

$$dC_b/dt = k_3 \cdot C_f - k_4 \cdot C_b.$$

In these equations C_f denotes the fraction of tissue ligand free to bind to receptor, C_a is the fraction of blood ligand free to cross the blood–brain barrier, and C_b is the fraction of tissue ligand bound to receptor. Whereas K_1 and k_2 describe the transport of ligand to brain and into brain tissue and back, the rate constants k_3 and k_4 relate to receptor-binding parameters (Fig. 1). This simple model obviously is only an approximation to reality, and even more complicated models have been developed but usually are too complex and poorly defined to be of practical use.

B_{max} denotes the concentration of receptors that are available for binding, k_{on} is the receptor–ligand association rate, k_{off} is the corresponding dissociation rate constant, and f_2 is the fraction of free ligand that is available for specific binding. As unlabeled ("cold") ligand is present in preparations of many radioligands, which compete for binding sites with the labeled tracer, the proportion of labeled tracer to total amount of injected ligand (specific activity, SA) must also be considered in the equations:

$$k_3 = k_{on} f_2 (B_{max} - [C_b/SA])$$

and

$$k_4 = k_{off}.$$

If the amount of total receptor-binding ligand, C_b/SA is very small relative to the binding capacity, B_{max}, it can be disregarded and k_3 is then simply the product of k_{on}, f_2, and B_{max}. With k_3 being constant in this linear model, a separation of receptor density (B_{max}) from the association kinetic constant (k_{on}) is not possible. If receptor occupancy by the ligand cannot be disregarded, k_3 is not constant and the individual variables and constants must be determined separately by complicated curve-fitting and analytic procedures. Only this complicated analysis, usually requiring multiple measurements with different SAs, provides quantitative measures of B_{max} and the dissociation constant (K_d) ($= k_{off}/k_{on}$) (*12*). In most clinical applications, no attempt is made to determine B_{max} and K_d separately but the binding potential ($BP = B_{max}/K_d$) is accepted as adequate (*13*). In the case of negligible occupancy of receptors by the tracer and coinjected cold ligand, the BP can be calculated from measured parameters of a kinetic study (*14*) as:

$$BP = K_1 k_3 / k_2 k_4 f_1.$$

Because accurate measurement of f_1 in plasma by clinical means is problematic, quite frequently a measure closely related to the BP, denoted BP′, is used. It assumes that nonspecific binding (as considered by f_2) in tissue is a constant and can, therefore, be disregarded. BP′ can be directly calculated from rate constants k_3 and k_4 by:

$$BP' = f_2 \cdot B_{max}/K_d = k_3/k_4.$$

Full kinetic fits to determine B_{max} and K_d are usually too complicated for routine use. Therefore, equilibrium approaches are applied to determine receptor binding. These compare the target region containing the receptor of interest and a reference region where tissue activity is free of specific receptor binding. Under equilibrium conditions the volumes of distribution can be obtained, typically by simple measurement of tissue activity C_b in target and reference region. Ideally, the 2 regions are different with respect to bound tracer C_b, but both contain the same activity of free tracer C_f. The modified binding potential (BP′) is related to the different distribution volumes, DV_{rec} in target tissue and DV_{ref} in reference tissue, and to the ratio between tissue activity (C_t) and free tracer activity:

$$BP' = (DV_{rec}/DV_{ref}) - 1 = (C_t/C_f) - 1.$$

Because it is often difficult to achieve actual equilibrium, an approximation is used from a graphic representation of kinetic data, the Logan plot (*15*) (Fig. 2): when the integral of regional activity over current regional activity is plotted versus the integral of plasma activity over regional activity, the slope of the curve approximates the regional tracer DV. By comparing the slopes for the target (DV_{rec}) and the reference region (DV_{ref}), the BP can be calculated. If it can be assumed that k_2 is not changed by the experiment in the target or reference region, it is even possible to avoid the

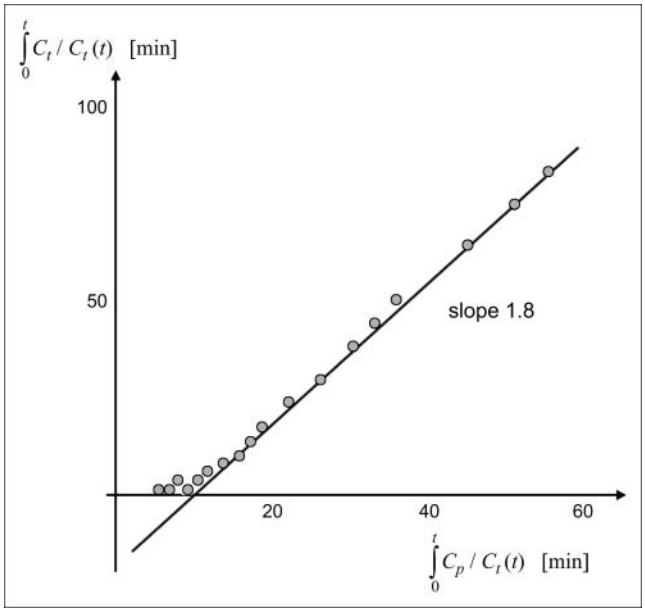

FIGURE 2. Schematic Logan plot for ligands that approach equilibrium during measurement time. By integral transformation of tissue and blood activity (as indicated at the axes), data points approach a straight line, whose slope equals BP′.

use of a plasma input function, and a transformed time axis involving the integral of tissue activity in the reference region is used. However, although the linear part of this plot approximates BP′, this convenient variant of the Logan plot must be used with caution because the results might be biased by changes in plasma binding or nonspecific tissue binding as well as changes in blood flow. Since the fitting in the Logan plot approach can be done by simple linear regression, this method is well suited for generation of parametric images.

RADIOLIGANDS FOR NEURORECEPTOR IMAGING BY PET AND SPECT

A large number of radioactive ligands labeled for receptors has been developed, but most of them were used only in vitro or in experimental animals and only few reached application in clinical nuclear medicine (*1,16*). For SPECT, most of the ligands tested in humans were labeled with ^{123}I (*17*). For PET, the ligands applied in humans were usually labeled with ^{11}C or ^{18}F (*18*) (Table 1).

DOPAMINE SYSTEM

Dopaminergic neurotransmission has a central role in many brain functions. It is necessary for proper movement coordination, and degeneration of the nigrostriatal dopamine system causes Parkinson's disease and is involved in multisystem atrophy. Pulsatile dopamine secretions elicit pleasant feeling and form a strong reward system that appears to play also a central role in drug abuse. The presynaptic nigrostriatal projection is the main location of the pathologic process in Parkinson's disease and, therefore, the assessment of disturbed dopamine synthesis is the main target for clinical studies (*19*). Postsynaptic receptors may also be involved in neurodegenerative disorders; they are functionally changed in the course of Parkinson's disease and by treatment with antiparkinson drugs, and they play an eminent role in schizophrenia and the effect of neuroleptics. There are 2 major dopamine receptor types (D_1 and D_2); the 3 other types (D_3, D_4, and D_5) detected in molecular genetic studies are related to these families—D_3 and D_4 are close to D_2 and D_5 is close to D_1. Only D_1 and D_2 receptors have been imaged in humans, but the applied radioligands usually bind also to the other subtypes.

Several preclinical and clinical studies have applied labeled benzazepines as potent and selective D_1 antagonists. Using these D_1 receptor tracers (^{11}C-SCH 23390, ^{11}C-NN112, and related compounds), the distribution of D_1 receptors known from autoradiographic investigations could be replicated by PET (striatum > kinetic regions = neocortex > thalamus) (*20*), and an age-dependent decrease (7% per decade) was observed (*21*). Studies with these radioligands indicated a significant decrease in D_1 receptor density in the striatum and frontal cortex of patients with bipolar affective disorders and in the prefrontal cortex of patients with schizophrenia (*22,23*). These tracers were also applied in competition studies to examine the binding of neuroleptic drugs to D_1 receptors (*24*) and for studies in Parkinson's disease.

There is a strong correlation between the antipsychotic potency of the classical neuroleptics and their in vitro affinity to and in vivo occupancy of D_2 receptors (*25,26*). Therefore, labeled neuroleptics were applied to map brain receptors, and the first visualization of receptors in living men was obtained with ^{11}C-*N*-methylspiperone (*27,28*). Several spiperone derivates, labeled for SPECT (^{77}Br-spiperone) or PET (^{11}C-*N*-methylspiperone, ^{76}Br-spiperone, ^{18}F-fluoroethylspiperone), have been introduced to image the physiologic and pathologic changes of the dopamine receptors in human striata. These tracers have a high affinity to D_2 receptors (K_d, 0.1 nmol/L) but also a high affinity to (5-hydroxytryptamine, 5-HT) 5-HT receptors, which are abundant in the cortex (*29*). Additionally, the binding of spiperone derivatives to D_2 receptors is very tight—essentially irreversible for practical reasons—allowing only saturation or competitive pretreatment studies. To permit equilibrium studies and facilitate replacement by other drugs, more specific D_2 ligands with higher selectivity to D_2 receptors, rapid association, and reversible binding were developed. The gold standard PET tracer for D_2 receptors today is the benzamide ^{11}C-raclopride (*30*), which has permitted the selective analysis of central D_2 receptors in primates and humans. For SPECT, ^{123}I-iodobenzamide is the most widely used D_2 receptor tracer (*31*). ^{11}C-Raclopride has a medium affinity to D_2 receptors (K_d, 1.2 nmol/L), is displaced more easily, and does not bind to 5-HT receptors. Benzamide derivatives with picomolar affinity—for example, ^{18}F-fallypride—are especially suitable for investigation of extrastriatal D_2 receptors (*32*). With these

tracers binding capacity is measured after equilibrium with plasma levels has been reached, making these tracers suitable to study receptor occupancy by neuroleptics or altered dopamine release.

These specific radioligands have been widely applied for the investigation of D_2 receptors in various physiologic conditions, in different neurologic and mental disorders, and in clinical pharmacology. The densities of D_2 receptors measured in vivo using equilibrium or kinetic models were comparable with the values from in vivo determinations, but differences in B_{max} between raclopride (30–40 nmol/L) and *N*-methylspiperone (15–25 nmol/L) were observed (*33,34*). A decrease of D_2 receptors with age has been observed in humans (*35*), and the D_2 receptor BP appears to be significantly lower in women than in men.

The binding capacity of striatal D_2 receptors is increased in idiopathic Parkinson's disease (Fig. 3). The increase is most pronounced in the posterior putamen, where the dopamine deficit is most severe, reflecting a change in receptor affinity (*36,37*). With progression of disease, striatal D_2 receptor activity returns to normal or even falls below the normal value (Fig. 3). However, agonist treatment affects receptor binding and possibly prevents supersensitivity phenomena expected in this disorder. After transplantation of medullar or fetal mesencephalic grafts to the putamen of patients with Parkinson's disease, no postoperative alteration of receptor density was observed despite some clinical improvements and increase in 6-fluoro-L-DOPA (FDOPA) uptake (*38*). Despite remarkable and long-lasting improvement of deficits during continuous high-frequency stimulation of basal nuclei, especially the subthalamic nucleus, a permanent effect on D_2 receptor activity was not observed (*39*). In progressive supranuclear palsy, a loss of striatal D_2 receptors, correlated with postmortem in vitro binding assays, has been reported (*40*). This loss of receptors was accompanied by a significant decrease in ^{18}F-labeled 3,4-dihydroxyphenylalanine (^{18}F-DOPA) uptake, indicating both pre- and postsynaptic neuronal degeneration. These findings support the role of D_2 receptor imaging in the differentiation of idiopathic Parkinson's disease from parkinsonian syndrome caused by multisystem atrophy (Fig. 3), which may account for up to 20% of cases presenting with parkinsonian symptoms. These patients, however, usually do not respond satisfactorily to treatment. The selective damage of postsynaptic striatal neurons can also be demonstrated by D_2 receptor imaging in Huntington's chorea, where presynaptic dopamine turnover is normal (*41,42*).

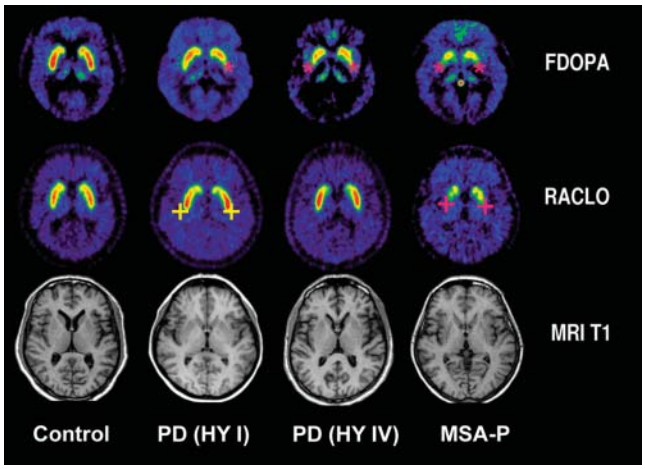

FIGURE 3. Comparison of dopamine synthesis and vesicular storage (^{18}F-labeled 6-fluoro-L-DOPA [^{18}F-FDOPA] PET, top row) and D_2 receptor binding (^{11}C-raclopride [RACLO] PET, middle row) in Parkinson's disease (PD) and multiple system atrophy with parkinsonian symptoms (MSA-P). FDOPA uptake is reduced in putamen in all conditions (red stars), whereas D_2 receptor binding is increased at an early stage of PET (HY stage I, yellow plus sign, second column), back to normal in advanced PD (HY stage IV, third column), and reduced in MSA-P (red plus sign, fourth column).

The findings with regard to D_2 receptor activity are controversial in schizophrenia. An increase in D_2 receptor binding capacity that was observed originally with ^{11}C-*N*-methylspiperone and competition with haloperidol (*43*) could not be replicated in drug-naïve patients with the more specific ligand raclopride (*33*). This controversy has not been entirely resolved, but the finding with spiperone seems not to be specific for schizophrenia (*44*). However, even when significant changes in striatal D_2 receptors could not be proven, changes of D_2 receptors in extrastriatal brain regions have been demonstrated, suggesting a relationship of positive symptoms with decreased D_2 receptor binding in the anterior cingulate cortex and in the thalamus (*45,46*).

In clinical pharmacology, specific labeling of striatal receptors with radioligands has been used to determine receptor occupancy during treatment with antipsychotic drugs. The classical neuroleptics occupy 60%–85% of striatal dopamine receptors at clinically effective doses (*47*). It has been estimated that antipsychotic action requires a receptor occupancy of 60%, whereas extrapyramidal side effects occur at ≥80% receptor occupancy (*48*). Overall, the results show an absence of direct correlations between D_2 receptor blockade and the disappearance or reappearance of psychotic symptoms. Additionally, long-lasting remission in schizophrenia patients after drug withdrawal was not related to persistent receptor occupation. However, even the most potent atypical neuroleptics—for example, clozapine and quietapine—show a lower occupancy of D_2 receptor than the typical antipsychotics with considerable interindividual variability (*49*). They may exert a more complex action on the imbalance of the dopaminergic system in schizophrenia—characterized by hyperstimulation of striatal D_2 receptors and understimulation of prefrontal D_1 receptors involving prefrontal glutamate transmission at *N*-methyl-D-aspartate (NMDA) receptors. The improved therapeutic efficacy of these atypical neuroleptics probably derives from a more moderate D_2 receptor blockade (hence, decreased extrapyramidal side effects) and increased prefrontal D_1 and NMDA-receptor transmission (*50*).

Binding of the reversible ligand raclopride to striatal D_2 receptors is sensitive to endogenous levels of dopamine and, therefore, the BP can be reduced by direct competition of the tracer with dopamine at the D_2 receptor. This effect can be used to study pharmacologic challenges (amphetamine, methylphenidate, cocaine, dopamine reuptake inhibitors, or tetrabenazine), which lead to increased synaptic levels of dopamine and, as a consequence, result in decreased raclopride binding. Changes in dopamine concentration and resulting raclopride binding, however, were also observed after a large variety of drugs—including ketamine, lorazepam, fenfluramine, nicotine, and alfentanil, to name a few—which do not all influence dopamine reuptake or synthesis directly but increase dopamine release indirectly via other complex neuronal circuits. Further studies in which dopamine release during physiologic activation can be assessed, as reduced raclopride binding, are of great interest and of importance: Functional stimulation by playing a video game (*51*) may elicit dopamine release, which can also be observed during repetitive transcortical magnetic stimulation of the prefrontal cortex, pointing to the close functional connections between these brain structures (*52*). The dopamine system is also activated by placebo infusion due to the expectation of improvement of extrapyramidal symptoms and pain (*53,54*) and as a reward system in substance abuse and addiction (*55*) as well as in obesity (*56*).

The neural dopamine transporter (DAT) is a membrane-bound presynaptically located protein that regulates the concentration of dopamine in nerve terminals. Several compounds have been shown to be antagonists of the monoamine reuptake system and, as nomifensine and substituted analogs of cocaine, they can be labeled for PET or SPECT studies (^{11}C-nomifensine, ^{11}C-cocaine, ^{11}C-methyl-phenidate, as well as the tropane-type derivatives of cocaine: ^{11}C and ^{123}I-CIT = 2β-carboxymethoxy-3β-(4-iodophenyl)tropane and ^{123}I- or ^{11}C-CIT-FE and CIT-FM as analogs) (*1,8*). Labeling of the reuptake sites with such tracers provides a measure of the density of dopaminergic nerve terminals. Studies in parkinsonian patients have demonstrated a reduction of the uptake of these tracers that correlated with the decrease in ^{18}F-DOPA uptake (Fig. 3). Therefore, these tracers can be used to demonstrate presynaptic involvement, especially in Parkinson's disease. Additionally, putamen and caudate were equally affected in multisystem atrophy, and a decrease of the transporter was also observed in Lesch–Nyhan disease. Other studies focused on drug abuse, where a relationship of the time course of the DAT blockade to cocaine abuse was found and a long-acting DAT inhibitor was postulated for antagonizing the pleasurable and additive effect of this drug (*57*).

SEROTONIN (5-HYDROXYTRYPTAMINE, 5-HT) SYSTEM

5-HT is the transmitter in the central nervous system involved in sleep, eating, sexual behavior, impulse control, circadian rhythm, and neuroendocine function, and it is also the precursor of the hormone melatonin. Serotonergic neurotransmission is altered in many neurologic and psychiatric disorders—in particular, in depression and compulsive disorders—but also in Alzheimer's and Parkinson's disease, autism, and schizophrenia. There is a great heterogeneity of the postsynaptic 5-HT receptors, which belong to 7 major classes and contain >16 subtypes. Suitable radioligands are only available for 5-HT_{1A} and 5-HT_{2A} receptors.

5-HT_{1A} receptors are present in high density in the hippocampus, septum, amygdale, hypothalamus, and neocortex of human brain. On stimulation, they open K^+ channels and in some areas also inhibit adenylate cyclase (*58*). Carbonyl-^{11}C-*N*-(2-[4-C2-methoxyphenyl]-1-piperazinyl)ethyl-*N*-(2-pyridinyl)cyclohexane carboxamide (^{11}C-WAY-100635, WAY) has high affinity for this receptor. ^{18}F-Labeled analogs of WAY (e.g., ^{18}F-*trans*-FCWAY) have been developed to increase clinical applicability, especially for replacement studies of the 5-HT_{1A} receptor as a functional target in new drug therapies. The affinity of ^{18}F-4-[2-methoxyphenyl]-1-(2-(*N*-2′-pirydynyl)-*p*-fluorobenzamido)ethylpiperazine (^{18}F-MPPF) is lower but, with a B_{max} of 2.9 pmol/mL and a K_d of 2.8 nmol/L in the hippocampal region, this radioligand might constitute an interesting tracer for the evaluation of endogenous 5-HT levels in limbic areas in health and disease and during drug therapy.

Abnormalities of 5-HT_{1A} receptors have been described in affective disorders, especially in depression, where a substantial reduction in BP was found in the raphe and in the mesotemporal cortex, and to a less extent also in the cortical areas (*59*); these changes are most prominent in bipolar depressives and in unipolar depressives with bipolar relatives. The reduction does not depend on previous treatment with 5-HT reuptake inhibitors (*60*). Some β-adrenergic receptor blockers that might be useful for augmentation of antidepressive therapy compete with 5-HT_{1A} ligands at the receptor. It must be kept in mind that displacement of ligands by a 5-HT agonist is age dependent and is also affected by anxiety (*61*).

5-HT_{2A} receptors are present in all neocortical regions, with lower densities in hippocampus, basal ganglia, and thalamus. The cerebellum and striatum of the brain stem are virtually devoid of 5-HT_{2A} receptors. A quantitation of 5-HT_{2A} receptors has been possible with ^{18}F-altanserin, ^{18}F-setoperone, and ^{123}I-2-ketanserin. These ligands are selective 5-HT_{2A} antagonists; they show good reproducibility. There is a sex difference in 5-HT_{2A} receptor density and a decrease in binding with age (*62*). Reduced 5-HT_{2A} receptor binding may be related to the pathophysiology of anorexia nervosa, as it remains affected long after weight restoration (*63*). There is also a significant binding of the D_2 receptor ligand ^{18}F-*N*-methylspiperone to 5-HT_{2A} receptors, which can be displaced by anxiolytic drugs (*64*).

The 5-HT transporter (5-HTT) belongs to the same family as the transporter for dopamine and norepinephine, all of which

provide reuptake of neurotransmitters into presynaptic neurons. Interest in 5-HTT is based on the essential role of the 5-HT system in depression (*65*) and the fact that tricyclic and nontricyclic antidepressants belong to the pharmacologic class of inhibitors of 5-HT reuptake, which enhance extracellular 5-HT levels. Many antidepressants were labeled, but their high lipophilicity induced high nonspecific binding in the brain and they have not been successful for PET or SPECT studies in humans.

PET of the 5-HTT sites has been possible with ^{11}C-McN5652 (hexahydro-6-[4-(methylthio)phenyl]pyrrolo-[2,1-a]-isoquinoline) but reliable quantification was obtained only in areas with high receptor density (midbrain, thalamus, striatum) (*66*). The 403U76 derivative ADAM exhibits high affinity and selectivity for 5-HTT and is an excellent SPECT tracer for visualization of 5-HTT in humans. ^{11}C-Labeled derivatives 3-amino-4-(2-dimethylaminomethylphenylsulfanyl)benzonitrile (DASP) and *N,N*-dimethyl-2-(2-amino-4-methylphenylthio)benzylamin (MADAM) exhibit high affinity and selectivity for 5-HTT and have proven to be excellent PET tracers for visualization of 5-HTT in human brains. These tracers are suitable for monitoring in vivo 5-HT levels (*67*). The BP of 5-HTT in the thalamus was significantly increased in patients with depression, whereas the BP in the midbrain was normal (*68*). The 5-HTT might also play a role in abuse of ecstasy (3,4-methylen-dioxymethamphetamine), as a long-standing reduction of 5-HTT density was observed after repeated application in baboons (*69*).

CHOLINERGIC SYSTEM

Acetylcholine receptors were originally subdivided into 2 main classes, nicotinic and muscarinic, but multiple heterogeneous subtypes have been characterized. Nicotinic receptors belong to the ligand-gated ion channels, and muscarinic receptors operate via several second messengers.

Nicotinic receptors have been implied in many psychiatric and neurologic diseases, including depression and cognitive and memory disorders, such as Alzheimer's and Parkinson's disease. Thus, ^{11}C-labeled nicotine was used to visualize and quantify nicotinic receptors in the brain. High binding was reported in several cortical and subcortical regions, and low density was found in the pons, cerebellum, occipital cortex, and white matter. Higher uptake was observed in smokers than in nonsmokers, indicating increased density of nicotinic binding with chronic administration of nicotine. However, the high nonspecific binding and its rapid washout have limited the clinical application of this tracer. More specific ligands, such as epibatidine and derivatives labeled with ^{11}C or ^{18}F, showed high uptake in thalamus and hypothalamus or midbrain, intermediate uptake in the neocortex and hippocampus, and low uptake in the cerebellum, which corresponds with the known distribution of nicotinic receptors (*70*).

Early in the course of Alzheimer's disease, a reduced uptake of radioligands to nicotinic receptors in frontal and temporal cortex has been observed in comparison with that of age-matched healthy control subjects (*71*). However, the quantitative measurement of the acetylcholinesterase activity in the brain by radiolabeled acetylcholine analogs (*N*-methyl-3-piperydyl-acetate [MP3A], *N*-methylpiperidin-4-yl-acetate [MP4A], and *N*-methylpiperidin-4-yl-propionate [PMP]) has found broader clinical application, because these tracers easily enter the brain, are selectively hydrolyzed, and then are trapped in the brain, permitting quantitation in a 2-tissue-compartment model (*72*). Studies in patients with Alzheimer's disease demonstrated a widespread reduction of acetylcholinesterase activity in the cerebral cortex (*73–75*) (Fig. 4) and allow differentiation of Parkinson's disease and progressive nuclear palsy. Additionally, the early loss of cholinergic transmission in the cortex could be shown with these tracers, which precedes the loss of cholinergic neurons in the nucleus basalis of Meynert (*76*) (Fig. 4). The inhibition of acetylcholinesterase, resulting from treatment with specific drugs, such as donepezil, can also be measured with these tracers (*77*).

Imaging muscarinic receptors, which are the dominant postsynaptic cholinergic receptors in the brain, has been pursued by many tracers for SPECT and PET (^{123}I- and ^{11}C-quinuclidinyl-benzylate [QNB], ^{11}C-2α-tropanyl-benzylate [TKB], ^{11}C-*N*-methylpiperidyl-benzylate [NMPB], ^{11}C-scopolamine, and ^{11}C-benztropine), but all of these radiopharmaceuticals lack selectivity for receptor subtypes. The highest binding for these ligands is usually found in the cortex, striatum, thalamus, and pons. Normal aging was

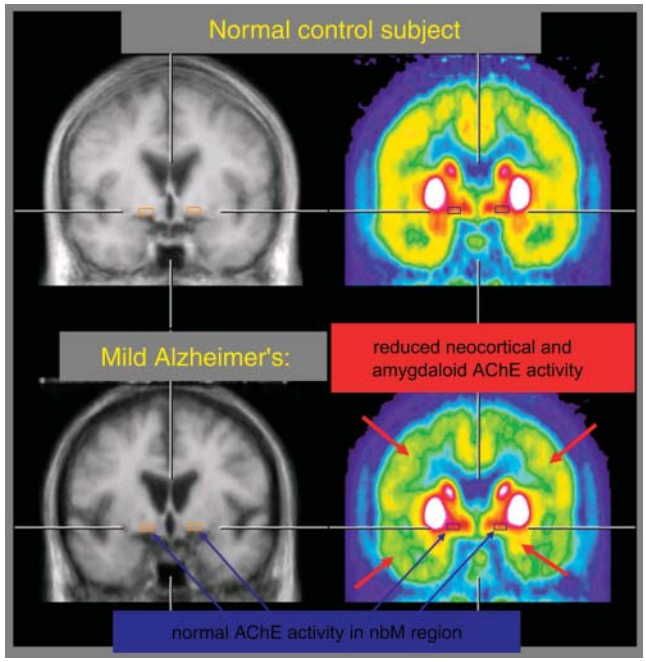

FIGURE 4. ^{11}C-MP4A PET in mild-to-moderate Alzheimer's disease demonstrates reduction in cortex and amygdala but preserved activity in basal forebrain, which suggests a dying-back of cholinergic neurons rather than initial loss of cell bodies. AChE = acetylcholinesterase; nbM = nucleus basalis of Meynert.

associated with reduction of muscarinic receptor binding in neocortical regions and thalamus (*78*). Whereas no regional changes were observed in Alzheimer's disease, hypersensitivity of muscarinic receptors was found in the frontal cortex of patients with Parkinson's disease.

γ-AMINOBUTYRIC ACID (GABA) SYSTEM

GABA is the most important inhibitory neurotransmitter. Its transmission is altered in epilepsy and is also altered in anxiety and other psychiatric disorders. Because the GABA receptor is abundant in the cortex and is very sensitive to damage, it represents a reliable marker of neuronal integrity—for example, in ischemic brain damage and in various neurodegenerative diseases. Part of the $GABA_A$ receptor complex, which gates the Cl^- channel, is the central benzodiazepine receptor, which specifically mediates all pharmacologic properties of the benzodiazepines (sedative, anxiolytic, anticonvulsant, myorelaxant). The tracer most widely used for central benzodiazepine-binding sites is the antagonist flumazenil labeled with ^{11}C or ^{123}I.

Because of low nonspecific binding, quantitation can be achieved in equilibrium by a rather simple 1-tissue-compartment model (*79*). Owing to a high extraction rate, initial tracer uptake represents regional cerebral perfusion, with subsequent rapid approximation of the DV that represents receptor binding. For clinical use to detect focal alterations in flumazenil activity, images obtained 10–20 min after injection are essentially equivalent to parametric images of the DV. A differentiation between receptor density and affinity can be achieved by kinetic analysis in combination with various amounts of unlabeled tracer.

The highest degree of binding is observed in the medial occipital cortex, followed by other cortical areas—the cerebellum, thalamus, striatum, and pons—with very low binding in the white matter (which can be used as a reference region). Flumazenil binding is age dependent, with highest values reached at approximately 2 y and a subsequent decline by 25%–50%, until adult values are reached at age 14–22 y (*80*). A partial inverse agonist, ^{11}C-labeled RO-15-4513, which binds preferentially to the α_5 receptor subtype, showed uptake that was greater in limbic areas—in particular, in the anterior cingulate cortex, hippocampus, and insular cortex—but lower in the occipital cortex and cerebellum in comparison with flumazenil, which binds mainly to the α_1 subtype (*81*). This compound could be of particular interest for studies of memory function and memory-enhancing drugs. In contrast to other receptors, this radioligand does not show an age-dependant effect on receptor binding.

In epilepsy, a reduced benzodiazepine receptor density has been demonstrated in epileptic foci, and flumazenil was found to be more sensitive and more accurate for focus localization than ^{18}F-FDG (*82,83*). Flumazenil is a biochemical marker of epileptogenicity and neuronal loss; benzodiazepine receptor-density changes are more sensitive than ^{18}F-FDG in detecting hippocampal sclerosis or microdysgenesis, and benzodiazepine receptor studies were useful in the selection of patients for targeted surgery and for predicting outcome of these procedures (*84,85*).

The benzodiazepine-binding sites are affected in a variety of degenerative disorders, indicating a loss of $GABA_A$ receptor–carrying neurons: This is the case in Huntington's disease, where a reduction in the benzodiazepine receptor density was observed in the caudate and putamen, which, however, was preceded by impairment of neuronal metabolism assessed by FDG (*86*). In progressive supranuclear palsy, the global reduction in benzodiazepine-binding sites in the cortex suggests loss of intrinsic neurons and is related to the cognitive impairment accompanying this disorder (*87*). In contrast, in early Alzheimer's disease, preserved benzodiazepine-binding sites relative to glucose hypometabolism suggests intact cortical neurons. In some cerebellar ataxias (e.g., SCA6), benzodiazepine receptor density in the cerebellum is reduced early in the course, indicating loss of cortical neurons (*88,89*). In patients with hepatic encephalopathy, an increase in cortical flumazenil binding was observed, which may account for the hypersensitivity to benzodiazepines observed in this disorder (*90*).

In ischemic stroke, flumazenil is used to detect irreversible tissue damage: it is the most sensitive early predictor of eventual ischemic infarction and, therefore, is useful for the selection of patients who can benefit from invasive therapeutic strategies (*91*). In subacute and chronic states after stroke, functional impairment without morphologic lesions on CT could be attributed to silent infarctions characterized by significant reduction of benzodiazepine binding (*92*).

In schizophrenia, a correlation between reduced benzodiazepine receptor binding in limbic cortical regions and psychotic symptoms was found (*93*). Reduced receptor binding in the temporal, occipital, and frontal lobes was also observed in panic and anxiety disorders (*65*).

Studies of brain receptor occupancy by different drugs acting at the benzodiazepine receptor sites have been used to demonstrate the pharmacologic activity of various benzodiazepines and to investigate noninvasively in vivo the activity of new anxiolytic, anticonvulsant, and sedative drugs in relation to their molecular interaction at the benzodiazepine receptor (*94*). These studies yield important insight into drug action, despite the fact that flumazenil-binding parameters in the neocortex and cerebellum were not found to be related to anxiety trait or state (*95*).

Another binding site for benzodiazepine in the brain is the peripheral-type receptor, which is not located on the membrane of neurons but, rather, in the mitochondrial and nuclear subcellular fraction. This peripheral benzodiazepine receptor may play a role in oxidative metabolism and ion fluxes. The tracer most frequently used as the ligand for the peripheral benzodiazepine receptor is the isoquinoline ^{11}C-PK-11195, which binds to activated, but not resting, microglia. It has been used as a marker of disease activity in inflammatory diseases, such as multiple sclerosis (*96*),

and as an indicator of glia–macrophage activation in ischemia (*97*), Alzheimer's disease (*98*), and brain tumors (*99*).

As an antagonist of GABA, glutamate is the main excitatory neurotransmitter in the cortex, and alterations of glutamatergic neurotransmission are associated with many neurologic diseases. At higher concentrations, glutamate has neurotoxic potential and is involved in the cascade of neuronal damage in ischemia and degenerative disorders. So far, the tracers used to study this system (^{11}C-MK 801, ^{18}F-fluoroethyl-TCP, ^{11}C-ketamine, and ^{18}F-memantine) have only a low specificity to the NMDA receptor, and relevance for clinical studies has not been established (*100*).

ADENOSINE RECEPTORS

The adenosine receptors (A_1 and A_{2A}) play a role in neuromodulation and are functionally altered in epilepsy, stroke, movement disorders, and schizophrenia. The labeled xanthine analogs ^{18}F-CPFPX and ^{11}C-MPDX are ligands for the A_1 receptor, which shows high density in the putamen and mediodorsal thalamus, intermediate density in most cortical regions, and low density in the midbrain, brain stem, and cerebellum (*101–103*). The A_{2A} receptors have also been visualized recently in human brain (*104*). These tracers might have a potential for prediction of severe tissue damage in early states of ischemic stroke.

OPIOID RECEPTORS

Morphine, codeine, heroin, and pethidine were labeled with ^{11}C but, because of the complex metabolism of these compounds and nonspecific binding, these tracers are not well suited for opioid receptor imaging. Successful PET tracers have been obtained with ^{11}C-carfentanyl, a potent synthetic μ opiate antagonist, and ^{11}C-diprenorphine and ^{18}F-cyclofoxy, which bind to all types of opioid receptors.

^{11}C-Carfentanyl, the ligand for the μ receptors, which are the primary site for pleasurable reward feeling, reaches the highest concentrations in the basal ganglia and thalamus (*105*). With ^{11}C-diprenorphine, the ligand for μ and non-μ–receptor sites, high naloxone-replaceable concentrations can be obtained in the striatum and in the cingulate and frontal cortex, including the cortical projections of the medial pain system (*106*). ^{18}F-Cyclofoxy, an antagonist to μ and k subtypes, is distributed similarly to the distribution of naloxone in the caudate, amygdala, thalamus, and brain stem. In some areas, opioid receptors are at a higher concentration in women, in whom also an age-related decline in receptor density was found (*107*).

In temporal lobe epilepsy, ^{11}C-carfentanyl binding was increased in the amygdala and temporal cortex, suggesting an upregulation of opioid receptors or decreased occupancy by endogenous peptides (*108*). Increased ^{11}C-carfentanyl binding was also observed with cocaine craving in addicted men (*109*).

The opioid receptor system plays a central role in perception and emotional processing of pain, and changes in receptor availability are related to chronic pain, suggesting increased endogenous release or downregulation of receptors (*110*).

Regional μ receptors were differentially regulated according to sensory and affective or emotional dimensions of pain (*111*), as decreased ^{11}C-carfentanyl BP varied directly with ratings of pain intensity. Decreased ^{11}C-diprenorphine binding during trigeminal neuralgic pain was also explained with increased occupancy by endogenous opioid peptides (*112*). In several degenerative disorders (Parkinson's disease, striatonigral degenerations, progressive supranuclear palsy, olivopontocerebellar atrophy, and Tourette's syndrome), the pattern of opioid receptor binding is altered (*113*).

Although there are numerous other ligands and other receptors in the human brain, this review concentrated on those that have already gained application in several centers and are thus beginning to have broader clinical impact. Further work on these tracers, and on the new ones to emerge, is likely to deeply influence development of new drugs and to provide highly specific diagnostic imaging for more effective treatment in clinical neurology.

CONCLUSION

Receptors have a central role in neurotransmission and neuromodulation and are involved in all brain functions, ranging from motor performance to memory, emotion, and pain. The imaging of the distribution, density, and activity of various receptors therefore permits insight into the physiologic activities of functional networks and their disturbance by neurologic and psychiatric disorders and can be used for studying selective drug action.

REFERENCES

1. Verhoeff NPLG. Ligands for neuroreceptor imaging by positron or single-photon emission computed tomography. In: Ell PJ, Gambhir SS, eds. *Nuclear Medicine in Clinical Diagnosis and Treatment.* Edinburgh, U.K.: Churchill Livingstone; 2004:1275–1294.
2. Zilles K, Palomero-Gallagher N, Schleicher A. Transmitter receptors and functional anatomy of the cerebral cortex. *J Anat.* 2004;205:417–432.
3. Kung HF. Overview of radiopharmaceuticals for diagnosis of central nervous disorders. *Crit Rev Clin Lab Sci.* 1991;28:269–286.
4. Young AB, Penney JB, Starosta-Rubinstein S, et al. PET scan investigations of Huntington's disease: cerebral metabolic correlates of neurological features and functional decline. *Ann Neurol.* 1986;20:296–303.
5. Lammertsma AA, Hume SP. Simplified reference tissue model for PET receptor studies. *Neuroimage.* 1996;4:153–158.
6. Gunn RN, Lammertsma AA, Hume SP, et al. Parametric imaging of ligand-receptor binding in PET using a simplified reference region model. *Neuroimage.* 1997;6:279–287.
7. Lammertsma AA. Radioligand studies: imaging and quantitative analysis. *Eur Neuropsychopharmacol.* 2002;12:513–516.
8. Huang S-C, Barrio JR, Phelps ME. Neuroreceptor assay with positron emission tomography: equilibrium versus dynamic approaches. *J Cereb Blood Flow Metab.* 1986;6:515–521.
9. Mazoyer BM. Investigation of the dopamine system with positron emission tomography: general issues in modelling. In: Baron J-C, Comar D, Farde L, Martinot J-L, Mazoyer B, eds. *Brain Dompaminergic Systems: Imaging with Positron Emission Tomography.* Dordrecht, The Nertherlands: Kluwer Academic Publishers; 1991:65–83.
10. Wienhard K. Application to the D2 receptors. In: Baron J-C, Comar D, Farde L, Martinot J-L, Mazoyer B, eds. *Brain Dopaminergic Systems: Imaging with*

Positron Emission Tomography. Dordrecht, The Netherlands: Kluwer Academic Publishers; 1991:85–95.
11. Herholz K, Herscovitch P, Heiss W-D. *NeuroPET: Positron Emission Tomography in Neuroscience and Clinical Neurology.* Berlin, Germany: Springer; 2004.
12. Delforge J, Spelle L, Bendriem B, et al. Parametric images of benzodiazepine receptor concentration using a partial-saturation injection. *J Cereb Blood Flow Metab.* 1997;17:343–355.
13. Mintun MA, Raichle ME, Kilbourn MR, et al. A quantitative model for the in vivo assessment of drug binding sites with positron emission tomography. *Ann Neurol.* 1984;15:217–227.
14. Meyer JH, Ichise M. Modeling of receptor ligand data in PET and SPECT imaging: a review of major approaches. *J Neuroimaging.* 2001;11:30–39.
15. Logan J, Fowler JS, Volkow ND, et al. Graphical analysis of reversible radioligand binding from time-activity measurements applied to [N-^{11}C-methyl]-(-)-cocaine PET studies in human subjects. *J Cereb Blood Flow Metab.* 1990;10:740–747.
16. Mazière M, Berger G, Comar D. ^{11}C-Radiopharmaceuticals for brain receptor studies. In: Lambrecht RM, Morcos N, eds. *Applications of Nuclear and Radiochemistry.* New York, NY: Pergamon Press; 1982:251–270.
17. Kung HF, Kung MP, Choi SR. Radiopharmaceuticals for single-photon emission computed tomography brain imaging. *Semin Nucl Med.* 2003;33:2–13.
18. Mazière B, Halldin C. PET tracers for brain scanning. In: Ell PJ, Gambhir SS, eds. *Nuclear Medicine in Clinical Diagnosis and Treatment.* Edinburgh, U.K.: Churchill Livingstone; 2004:1295–1329.
19. Heiss W-D, Hilker R. The sensitivity of 18-fluorodopa positron emission tomography and magnetic resonance imaging in Parkinson's disease. *Eur J Neurol.* 2004;11:5–12.
20. Abi-Dargham A, Martinez D, Mawlawi O, et al. Measurement of striatal and extrastriatal dopamine D1 receptor binding potential with [^{11}C]NNC 112 in humans: validation and reproducibility. *J Cereb Blood Flow Metab.* 2000;20:225–243.
21. Wang Y, Chan GLY, Holden JE, et al. Age-dependent decline of dopamine D1 receptors in human brain: a PET study. *Synapse.* 1998;30:56–61.
22. Suhara T, Nakayama K, Inoue O, et al. D1 dopamine receptor binding in mood disorders measured by positron emission tomography. *Psychopharmacology (Berl).* 1992;106:14–18.
23. Okubo Y, Suhara T, Suzuki K, et al. Decreased prefrontal dopamine D1 receptors in schizophrenia revealed by PET. *Nature.* 1997;385:634–636.
24. Nordstrom AL, Farde L, Nyberg S, et al. D1, D2, and 5-HT2 receptor occupancy in relation to clozapine serum concentration: a PET study of schizophrenic patients. *Am J Psychiatry.* 1995;152:1444–1449.
25. Nordstrom AL, Farde L, Wiesel FA, et al. Central D2-dopamine receptor occupancy in relation to antipsychotic drug effects: a double-blind PET study of schizophrenic patients. *Biol Psychiatry.* 1993;33:227–235.
26. Wiesel FA, Farde L, Nordstrom AL, et al. Central D1- and D2-receptor occupancy during antipsychotic drug treatment. *Prog Neuropsychopharmacol Biol Psychiatry.*1990;14:759–767.
27. Wong DF, Gjedde A, Wagner HN Jr. Quantification of neuroreceptors in living human brain. I. Irreversible binding of ligands. *J Cereb Blood Flow Metab.* 1986;6:137–146.
28. Wagner HN Jr, Burns HD, Dannals RF, et al. Assessment of dopamine receptor densities in the human brain with carbon-11-labeled N-methylspiperone. *Ann Neurol.* 1984;15(suppl):S79–S84.
29. Nyberg S, Farde L, Eriksson L, et al. 5-HT$_2$ and D$_2$ dopamine receptor occupancy in the living human brain: a PET study with risperidone. *Psychopharmacology (Berl).* 1993;110:265–272.
30. Farde L, Pauli S, Hall H, et al. Stereoselective binding of ^{11}C-raclopride in living human brain: a search for extrastriatal central D2-dopamine receptors by PET. *Psychopharmacology (Berl).* 1988;94:471–478.
31. Verhoeff NPLG. *Neuroreceptor Ligand Imaging by Single Photon Emission Computerized Tomography (SPECT)* [thesis]. Amsterdam, The Netherlands: University of Amsterdam; 1993.
32. Mukherjee J, Christian BT, Dunigan KA, et al. Brain imaging of ^{18}F-fallypride in normal volunteers: blood analysis, distribution, test-retest studies, and preliminary assessment of sensitivity to aging effects on dopamine D-2/D-3 receptors. *Synapse.* 2002;46:170–188.
33. Farde L, Wiesel FA, Stone-Elander S, et al. D$_2$ dopamine receptors in neuroloptic-naive schizophrenic patients: a positron emission tomography study with (^{11}C)raclopride. *Arch Gen Psychiatry.* 1990;47:213–219.
34. Wong DF, Gjedde A, Wagner HN Jr, et al. Quantification of neuroreceptors in the living human brain. II. Inhibition studies of receptor density and affinity. *J Cereb Blood Flow Metab.* 1986;6:147–153.
35. Antonini A, Leenders KL, Reist H, et al. Effect of age on D$_2$ dopamine receptors in normal human brain measured by positron emission tomography and ^{11}C-raclopride. *Arch Neurol.* 1993;50:474–480.
36. Antonini A, Vontobel P, Psylla M, et al. Complementary positron emission tomographic studies of the striatal dopaminergic system in Parkinson's disease. *Arch Neurol.* 1995;52:1183–1190.
37. Hume SP, Opacka-Juffry J, Myers R, et al. Effect of L-dopa and 6-hydroxydopamine lesioning on [^{11}C]raclopride binding in rat striatum, quantified using PET. *Synapse.* 1995;21:45–53.
38. Cochen V, Ribeiro MJ, Nguyen JP, et al. Transplantation in Parkinson's disease: PET changes correlate with the amount of grafted tissue. *Mov Disord.* 2003;18:928–932.
39. Strafella AP, Sadikot AF, Dagher A. Subthalamic deep brain stimulation does not induce striatal dopamine release in Parkinson's disease. *Neuroreport.* 2003;14:1287–1289.
40. Baron JC, Maziere B. Loc'h C, Sgouropoulos P, Bonnet AM, Agid Y. Progressive supranuclear palsy: loss of striatal dopamine receptors demonstrated in vivo by positron tomography. *Lancet.* 1985;1:1163–1164.
41. Ginovart N, Lundin A, Farde L, et al. PET study of the presynaptic and postsynaptic dopaminergic markers for the neurodegenerative process in Huntington's disease. *Brain.* 1997;120:503–514.
42. Piccini P. Neurodegenerative movement disorders: the contribution of functional imaging. *Curr Opin Neurol.* 2004;17:459–466.
43. Wong DF, Wagner HN Jr, Tune LE, et al. Positron emission tomography reveals elevated D$_2$ dopamine receptors in drug-naive schizophrenics. *Science.* 1986;234:1558–1563.
44. Pearlson GD, Wong DF, Tune LE, et al. In vivo D2 dopamine receptor density in psychotic and nonpsychotic patients with bipolar disorder. *Arch Gen Psychiatry.* 1995;52:471–477.
45. Suhara T, Okubo Y, Yasuno F, et al. Decreased dopamine D2 receptor binding in the anterior cingulate cortex in schizophrenia. *Arch Gen Psychiatry.* 2002;59:25–30.
46. Talvik M, Nordstrom AL, Olsson H, et al. Decreased thalamic D2/D3 receptor binding in drug-naive patients with schizophrenia: a PET study with [^{11}C]FLB 457. *Int J Neuropsychopharmacol.* 2003;6:361–370.
47. Farde L, Wiesel F-A, Halldin C, Sedvall G. Central D2-dopamine receptor occupancy in schizophrenic patients treated with antipsychotic drugs. *Arch Gen Psychiatry.* 1988;45:71–76.
48. Remington G, Chong SA, Kapur S. Distinguishing change in primary and secondary negative symptoms. *Am J Psychiatry.* 1999;156:974–975.
49. Talvik M, Nordstrom AL, Nyberg S, et al. No support for regional selectivity in clozapine-treated patients: a PET study with [^{11}C]raclopride and [^{11}C]FLB 457. *Am J Psychiatry.* 2001;158:926–930.
50. Abi-Dargham A, Laruelle M. Mechanisms of action of second generation antipsychotic drugs in schizophrenia: insights from brain imaging studies. *Eur Psychiatry.* 2005;20:15–27.
51. Koepp MJ, Gunn RN, Lawrence AD, et al. Evidence for striatal dopamine release during a video game. *Nature.* 1998;393:266–268.
52. Strafella AP, Paus T, Barrett J, et al. Repetitive transcranial magnetic stimulation of the human prefrontal cortex induces dopamine release in the caudate nucleus. *J Neurosci.* 2001;21:RC157:1–4.
53. de la Fuente-Fernandez R, Schulzer M, Stoessl AJ. The placebo effect in neurological disorders. *Lancet Neurol.* 2002;1:85–91.
54. Colloca L, Benedetti F. Placebos and painkillers: Is mind as real as matter? *Nat Rev Neurosci.* 2005;6:545–552.
55. Volkow ND, Fowler JS, Wang GJ. Role of dopamine in drug reinforcement and addiction in humans: results from imaging studies. *Behav Pharmacol.* 2002;13:355–366.
56. Wang GJ, Volkow ND, Thanos PK, et al. Similarity between obesity and drug addiction as assessed by neurofunctional imaging: a concept review. *J Addict Dis.* 2004;23:39–53.
57. Volkow ND, Wang GJ, Fischman MW, et al. Relationship between subjective effects of cocaine and dopamine transporter occupancy. *Nature.* 1997;386:827–830.
58. Passchier J. van Waarde A. Visualisation of serotonin-1A (5-HT1A) receptors in the central nervous system. *Eur J Nucl Med.* 2001;28:113–129.
59. Drevets WC, Frank E, Price JC, et al. Serotonin type-1A receptor imaging in depression. *Nucl Med Biol.* 2000;27:499–507.
60. Sargent PA, Kjaer KH, Bench CJ, et al. Brain serotonin1A receptor binding measured by positron emission tomography with [^{11}C]WAY-100635: effects of depression and antidepressant treatment. *Arch Gen Psychiatry.* 2000;57:174–180.
61. Tauscher J, Bagby RM, Javanmard M, et al. Inverse relationship between serotonin 5-HT(1A) receptor binding and anxiety: a [^{11}C]WAY-100635 PET investigation in healthy volunteers. *Am J Psychiatry.* 2001;158:1326–1328.
62. Sheline YI, Mintun MA, Moerlein SM, et al. Greater loss of 5-HT$_{2A}$ receptors in midlife than in late life. *Am J Psychiatry.* 2002;159:430–435.
63. Stamatakis EA, Hetherington MM. Neuroimaging in eating disorders. *Nutr Neurosci.* 2003;6:325–334.

64. Kanerva H, Vilkman H, Nagren K, et al. Brain 5-HT2A receptor occupancy of deramciclane in humans after a single oral administration: a positron emission tomography study. *Psychopharmacology (Berl).* 1999;145:76–81.
65. Malizia AL. Anxiety disorders and affective disorders. In: Ell PJ, Gambhir SS, eds. *Nuclear Medicine in Clinical Diagnosis and Treatment.* Edinburgh, U.K.: Churchill Livingstone; 2004:1399–1416.
66. Parsey RV, Kegeles LS, Hwang DR, et al. In vivo quantification of brain serotonin transporters in humans using [^{11}C]McN 5652. *J Nucl Med.* 2000; 41:1465–1477.
67. Ginovart N, Wilson AA, Meyer JH, et al. [^{11}C]-DASB, a tool for in vivo measurement of SSRI-induced occupancy of the serotonin transporter: PET characterization and evaluation in cats. *Synapse.* 2003;47:123–133.
68. Ichimiya T, Suhara T, Sudo Y, et al. Serotonin transporter binding in patients with mood disorders: a PET study with [^{11}C](+)McN5652. *Biol Psychiatry.* 2002;51:715–722.
69. Scheffel U, Szabo Z, Mathews WB, et al. In-vivo detection of short-term and long-term MDMA neurotoxicity: a positron emission tomography study in the living baboon brain. *Synapse.* 1998;29:183–192.
70. Villemagne VL, Horti A, Scheffel U, et al. Imaging nicotinic acetylcholine receptors with fluorine-18-FPH, an epibatidine analog. *J Nucl Med.* 1997;38: 1737–1741.
71. Nordberg A, Lundqvist H, Hartvig P, et al. Kinetic analysis of regional (S)(-) ^{11}C-nicotine binding in normal and Alzheimer brains: in vivo assessment using positron emission tomography. *Alzheimer Dis Assoc Disord.* 1995;9:21–27.
72. Koeppe RA, Frey KA, Snyder SE, et al. Kinetic modeling of N-[^{11}C]methylpiperidin-4-yl propionate: alternatives for analysis of an irreversible positron emission tomography tracer for measurement of acetylcholinesterase activity in human brain. *J Cereb Blood Flow Metab.* 1999;19:1150–1163.
73. Iyo M, Namba H, Fukushi K, et al. Measurement of acetylcholinesterase by positron emission tomography in the brains of healthy controls and patients with Alzheimer's disease. *Lancet.* 1997;349:1805–1809.
74. Kuhl DE, Koeppe RA, Minoshima S, et al. In vivo mapping of cerebral acetylcholinesterase activity in aging and Alzheimer's disease. *Neurology.* 1999;52:691–699.
75. Shinotoh H, Namba H, Yamaguchi M, et al. Positron emission tomographic measurement of acetylcholinesterase activity reveals differential loss of ascending cholinergic systems in Parkinson's disease and progressive supranuclear palsy. *Ann Neurol.* 1999;46:62–69.
76. Herholz K, Weisenbach S, Zündorf G, et al. In vivo study of acetylcholine esterase in basal forebrain, amygdala, and cortex in mild to moderate Alzheimer disease. *Neuroimage.* 2004;21:136–143.
77. Kuhl DE, Minoshima S, Frey KA, et al. Limited donepezil inhibition of acetylcholinesterase measured with positron emission tomography in living Alzheimer cerebral cortex. *Ann Neurol.* 2000;48:391–395.
78. Zubieta JK, Koeppe RA, Frey KA, et al. Assessment of muscarinic receptor concentrations in aging and Alzheimer disease with [^{11}C]NMPB and PET. *Synapse.* 2001;39:275–287.
79. Koeppe RA, Holthoff VA, Frey KA, et al. Compartmental analysis of [^{11}C]flumazenil kinetics for the estimation of ligand transport rate and receptor distribution using positron emission tomography. *J Cereb Blood Flow Metab.* 1991;11:735–744.
80. Chugani DC, Muzik O, Juhasz C, et al. Postnatal maturation of human GABAA receptors measured with positron emission tomography. *Ann Neurol.* 2001;49: 618–626.
81. Maeda J, Suhara T, Kawabe K, et al. Visualization of alpha5 subunit of GABAA/benzodiazepine receptor by ^{11}C Ro15-4513 using positron emission tomography. *Synapse.* 2003;47:200–208.
82. Savic I, Ingvar M, Stone-Elander S. Comparison of [^{11}C] flumazenil and [^{18}F] FDG as PET markers of epileptic foci. *J Neurol Neurosurg Psychiatry.* 1993; 56:615–621.
83. Szelies B, Sobesky J, Pawlik G, et al. Impaired benzodiazepine receptor binding in peri-lesional cortex of patients with symptomatic epilepsies studies by [C-11]-flumazenil PET. *Eur J Neurol.* 2002;9:137–142.
84. Juhasz C, Chugani DC, Muzik O, et al. Relationship of flumazenil and glucose PET abnormalities to neocortical epilepsy surgery outcome. *Neurology.* 2001; 56:1650–1658.
85. Richardson MP, Koepp MJ, Brooks DJ, et al. Benzodiazepine receptors in focal epilepsy with cortical dysgenesis: an C-11 flumazenil PET study. *Ann Neurol.* 1996;40:188–198.
86. Holthoff VA, Koeppe RA, Frey KA, et al. Positron emission tomography measures of benzodiazepine receptors in Huntington's disease. *Ann Neurol.* 1993;34:76–81.
87. Foster NL, Minoshima S, Johanns J, et al. PET measures of benzodiazepine receptors in progressive supranuclear palsy. *Neurology.* 2000;54:1768–1773.
88. Gilman S, Koeppe RA, Junck L, et al. Benzodiazepine receptor binding in cerebellar degenerations studied with positron emission tomography. *Ann Neurol.* 1995;38:176–185.
89. Jacobs AH, Kracht LW, Gossmann A, et al. Imaging in neurooncology. *NeuroRx.* 2005;2:333–347.
90. Samson Y, Bernuau J, Pappata S, et al. Cerebral uptake of benzodiazepine measured by positron emission tomography in hepatic encephalopathy. *N Engl J Med.* 1987;316:414–415.
91. Heiss W-D, Grond M, Thiel A, et al. Permanent cortical damage detected by flumazenil positron emission tomography in acute stroke. *Stroke.* 1998;29: 454–461.
92. Nakagawara J, Sperling B, Lassen NA. Incomplete brain infarction of reperfused cortex may be quantitated with iomazenil. *Stroke.* 1997;28:124–132.
93. Busatto GF, Pilowsky LS, Costa DC, et al. Correlation between reduced in vivo benzodiazepine receptor binding and severity of psychotic symptoms in schizophrenia. *Am J Psychiatry.* 1997;154:56–63.
94. Shinotoh H, Iyo M, Yamada T, et al. Detection of benzodiazepine receptor occupancy in the human brain by positron emission tomography. *Psychopharmacology (Berl).* 1989;99:202–207.
95. Abadie P, Boulenger JP, Benali K, et al. Relationships between trait and state anxiety and the central benzodiazepine receptor: a PET study. *Eur J Neurosci.* 1999;11:1470–1478.
96. Banati RB, Newcombe J, Gunn RN, et al. The peripheral benzodiazepine binding site in the brain in multiple sclerosis: quantitative in vivo imaging of microglia as a measure of disease activity. *Brain.* 2000;123:2321–2337.
97. Pappata S, Levasseur M, Gunn RN, et al. Thalamic microglial activation in ischemic stroke detected in vivo by PET and [^{11}C]PK1195. *Neurology.* 2000;55:1052–1054.
98. Groom GN, Junck L, Foster NL, et al. PET of peripheral benzodiazepine binding-sites in the microgliosis of Alzheimer's disease. *J Nucl Med.* 1995;36:2207–2210.
99. Black KL, Ikezaki K, Toga AW. Imaging of brain tumors using peripheral benzodiazepine receptor ligands. *J Neurosurg.* 1989;71:113–118.
100. Bressan RA, Pilowsky LS. Imaging the glutamatergic system in vivo: relevance to schizophrenia. *Eur J Nucl Med.* 2000;27:1723–1731.
101. Bauer A, Holschbach MH, Meyer PT, et al. In vivo imaging of adenosine A1 receptors in the human brain with [^{18}F]CPFPX and positron emission tomography. *Neuroimage.* 2003;19:1760–1769.
102. Fukumitsu N, Ishii K, Kimura Y, et al. Adenosine A1 receptor mapping of the human brain by PET with 8-dicyclopropylmethyl-1-^{11}C-methyl-3-propylxanthine. *J Nucl Med.* 2005;46:32–37.
103. Kimura Y, Ishii K, Fukumitsu N, et al. Quantitative analysis of adenosine A1 receptors in human brain using positron emission tomography and [1-methyl-^{11}C]8-dicyclopropylmethyl-1-methyl-3-propylxanthine. *Nucl Med Biol.* 2004;31:975–981.
104. Ishiwata K, Mizuno M, Kimura Y, et al. Potential of [^{11}C]TMSX for the evaluation of adenosine A2A receptors in the skeletal muscle by positron emission tomography. *Nucl Med Biol.* 2004;31:949–956.
105. Frost JJ, Wagner HN Jr, Dannals RF, et al. Imaging opiate receptors in the human brain by positron tomography. *J Comput Assist Tomogr.* 1985;9:231–236.
106. Sadzot B, Price JC, Mayberg HS, et al. Quantification of human opiate receptor concentration and affinity using high and low specific activity [^{11}C] diprenorphine and positron emission tomography. *J Cereb Blood Flow Metab.* 1991;11: 204–219.
107. Cohen RM, Carson RE, Sunderland T. Opiate receptor avidity in the thalamus is sexually dimorphic in the elderly. *Synapse.* 2000;38:226–229.
108. Mayberg HS, Sadzot B, Meltzer CC, et al. Quantification of mu and non-mu-opiate receptors in temporal lobe epilepsy using positron emission tomography. *Ann Neurol.* 1991;30:3–11.
109. Zubieta JK, Gorelick DA, Stauffer R, et al. Increased mu-opioid receptor binding detected by PET in cocaine-dependent men is associated with cocaine craving. *Nat Med.* 1996;2:1225–1229.
110. Sprenger T, Berthele A, Platzer S, et al. What to learn from in vivo opioidergic brain imaging? *Eur J Pain.* 2005;9:117–121.
111. Zubieta JK, Smith YR, Bueller JA, et al. Regional mu opioid receptor regulation of sensory and affective dimensions of pain. *Science.* 2001;293: 311–315.
112. Jones AK, Kitchen ND, Watabe H, et al. Measurement of changes in opioid receptor binding in vivo during trigeminal neuralgic pain using [^{11}C] diprenorphine and positron emission tomography. *J Cereb Blood Flow Metab.* 1999;19:803–808.
113. Burn DJ, Rinne JO, Quinn NP, et al. Striatal opioid receptor binding in Parkinson's disease, striatonigral degeneration and Steele-Richardson-Olszewski syndrome: a [^{11}C] diprenorphine PET study. *Brain.* 1995;118:951–958.

JNM The Journal of NUCLEAR MEDICINE

Brain Receptor Imaging

Wolf-Dieter Heiss and Karl Herholz

J Nucl Med. 2006;47:302-312.

The Journal of Nuclear Medicine is published monthly.
SNMMI | Society of Nuclear Medicine and Molecular Imaging
1850 Samuel Morse Drive, Reston, VA 20190.
(Print ISSN: 0161-5505, Online ISSN: 2159-662X)

SNMMI SOCIETY OF NUCLEAR MEDICINE AND MOLECULAR IMAGING